High strain rate characterization of polymers

Clive R. Siviour

Citation: AIP Conference Proceedings **1793**, 060029 (2017); doi: 10.1063/1.4971585
View online: http://dx.doi.org/10.1063/1.4971585
View Table of Contents: http://aip.scitation.org/toc/apc/1793/1
Published by the American Institute of Physics

High Strain Rate Characterization of Polymers

Clive R. Siviour[1, 2, a)]

[1] Department of Engineering Science, University of Oxford, Parks Road, Oxford, OX1 3PJ
[2] Pembroke College, Oxford, OX1 1DW

[a)] Corresponding author: clive.siviour@eng.ox.ac.uk

Abstract. This paper reviews the literature on the response of polymers to high strain rate deformation. The main focus is on the experimental techniques used to characterize this response. The paper includes a small number of examples as well as references to experimental data over a wide range of rates, which illustrate the key features of rate dependence in these materials; however this is by no means an exhaustive list. The aim of the paper is to give the reader unfamiliar with the subject an overview of the techniques available with sufficient references from which further information can be obtained. In addition to the 'well established' techniques of the Hopkinson bar, Taylor Impact and Transverse impact, a discussion of the use of time-temperature superposition in interpreting and experimentally replicating high rate response is given, as is a description of new techniques in which mechanical parameters are derived by directly measuring wave propagation in specimens; these are particularly appropriate for polymers with low wave speeds. The vast topic of constitutive modelling is deliberately excluded from this review.

INTRODUCTION

Accurate information about the mechanical response of polymers when subjected to high rate deformation is required in a wide range of applications. Polymers and their composites are increasingly being used to manufacture components that must safely withstand impact loading, or to act as energy absorbers / load mitigators to protect other sensitive devices. Here, they may be designed for one-off events in which plastic deformation is acceptable, or for repeated loadings in which the polymer must be able to return to its original dimensions and properties.

It is well known that the mechanical response of polymers is highly dependent on the applied loading frequency: the implication of this for monotonic large strain loading is that it is not sufficient to use properties measured under static loads in analysis of dynamic events (see Fig. 1 and examples in [1-6]). Moreover, the frequency dependence is not constant, but for any given polymer is greatest over the range(s) of frequencies corresponding to polymer transition(s) at the test temperature. Furthermore, it has long been known that the effects of frequency and temperature are interlinked through the well-known time-temperature superposition principle, Fig. 2: changes in one can be related to changes in the other through shift factors [7]. Hence, just as a survey of mechanical properties at a single frequency or loading rate displays particularly rapid changes at various transition temperatures (e.g. the glass transition), a survey of mechanical properties at a single temperature displays the same changes, due to the same underlying microstructural processes, at various frequencies; this is discussed further below.

As well as the requirement to better use polymers in industrial applications, there are other reasons for measuring their high rate properties: the rate dependence in many composites is due to, and similar in form to, that of the matrix polymer; the responses of many biomaterials are similar to rubbery polymers (and the challenges in measuring behavior are the same); and dynamic loading probes aspects of material response which are not 'visible' in quasi-static loading and therefore gives physical insights into the material structure and properties.

However, performing measurements of polymer behavior at high rates can be challenging, and the very properties which make them useful contribute to this challenge. Over a given range of temperatures and rates, a single polymer may exhibit a wide range of mechanical responses, from rubbery to ductile plastic to brittle (e.g. [6, 8-13]). Compared to most metals, the modulus is low (say 100 MPa for rubber, 2 GPa for Polycarbonate, 210 GPa for Steel), and although the density is also lower, the wave speed, which scales as $(E/\rho)^{1/2}$, can be as much as a thousand

Shock Compression of Condensed Matter - 2015
AIP Conf. Proc. 1793, 060029-1–060029-12; doi: 10.1063/1.4971585
Published by AIP Publishing. 978-0-7354-1457-0/$30.00

times lower for a soft polymer than for a metal, Fig. 3. Hence, if a dynamic stress or velocity profile is applied to one end of a polymer specimen it may take a significant period of time to reach the other end. Effectively, the characteristic time period for wave oscillation in the specimen becomes comparable to the duration of the loading, so that the specimen rings up. Thus, time must be allowed for the forces at each end to equilibrate. This is a particular problem for elastomers with very low wave speeds and brittle polymers that demonstrate small strains to failure [14]. The requirement for these oscillations to 'die down' so that the specimen is in static equilibrium is a key factor in discussions of the reliability of data obtained from possibly the most common technique used to measure dynamic properties of materials, the split-Hopkinson bar (see below). A further complication for many polymers, such as rubbers, is that they can exhibit very large, recoverable, deformations, and for hyperelastic materials experimental measurements over large strains may be required to characterize the strain hardening [15].

A further challenge, common to all materials, is the lack of diagnostics with high enough acquisition speeds to characterize the structural response of a specimen to high rate deformation: for a strain rate of 1000 s^{-1}, if data are required every 1% strain, an acquisition time of 10 μs or better is required. High speed photography and X-ray diffraction can operate at sufficient speeds. Thermal imaging is difficult, only recently have thermal cameras with suitable acquisition times become available [19-21] (a commercial camera is now available with 64×4 pixels at 100k fps, see also [22, 23]). This is in contrast to the range of techniques that can be used for in-situ structural measurements at low rates of strain (e.g. SEM, ESEM, X-ray Tomography, X-ray diffraction etc).

ESTABLISHED TECHNIQUES FOR HIGH RATE PROPERTIES

It has long been known that the dynamic properties of materials differ from those under static loading, and since the pioneering work of the Hopkinsons, numerous techniques have developed to measure these properties. Any such technique must be able to deliver the mechanical load or deformation to the specimen, and then transmit suitable information from the specimen to instrumentation that allows forces and deformations to be calculated. An overview of experimental methods is given in a review by Field *et al.* [18]; the current paper will focus on key techniques for polymers, in particular for the 'High Rate' range, from about 100 to 10,000 s^{-1}, see Fig. 4.

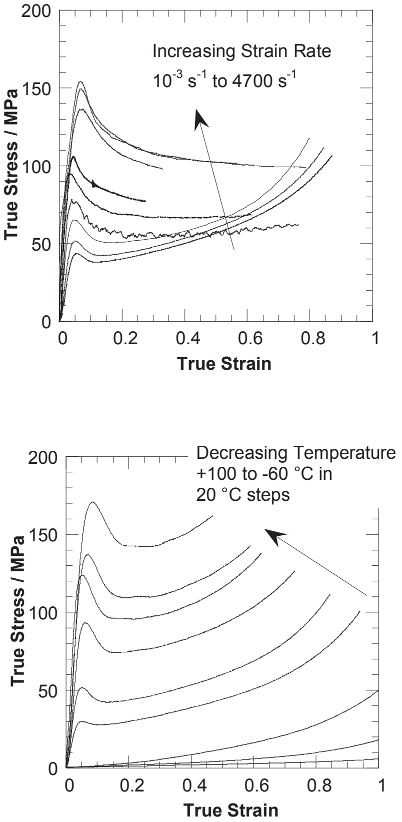

FIGURE 1. The mechanical response of PVC, like most polymers, is dependent on strain rate and temperature [17].

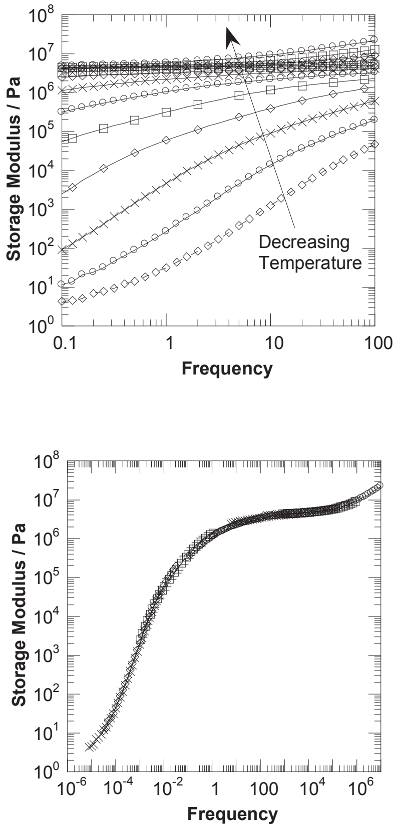

FIGURE 2. Time-temperature superposition allows a master curve to be constructed.

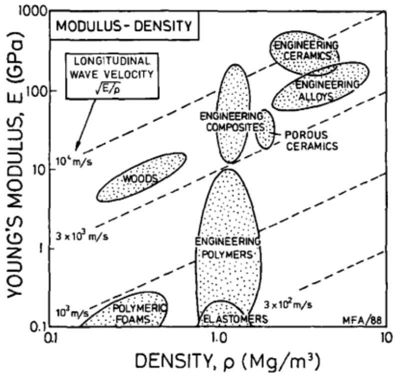

FIGURE 3. Modulus - density [16].

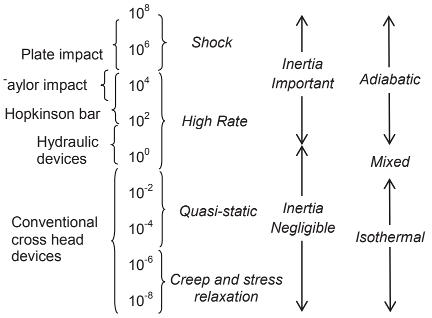

FIGURE 4. Testing techniques and experimental considerations at different strain rates, after [18].

The split-Hopkinson bar

The split-Hopkinson bar, Fig. 5 is a widely used apparatus for high strain rate characterization in compression, tension and torsion, and is well-described in the literature [24-27]. In the compression system a cylindrical specimen, dimensions of order 1 – 10 mm, is sandwiched between two slender metal rods, which are instrumented with strain gages. A gas gun is used to propel a third, striker, rod, which on impact introduces an incident stress wave. On arriving at the specimen, some of this wave is reflected and some transmitted. From measurements of these waves, the forces and displacements at the specimen-rod interface can be calculated; and if the specimen is in static equilibrium (the forces on the two ends are the same) its stress-strain response may be derived.

For low wave speed materials, the equilibrium assumption must be considered carefully, amongst other challenges [28]. The stress wave oscillates in the specimen and causes its stress to rise in a stepwise manner [29, 30]. Indeed, whilst the very first published papers describing the split-Hopkinson bar presented data on polymers, very thin specimens were used for this reason [31, 32]. For rubbers, the very low stiffness (or strength) to density ratio can also lead to artifacts from the *lateral* inertia of the specimen, especially for large specimens [33, 34]. The main cause of this is the rapid acceleration during the initial rise of the input pulse, before constant strain rate deformation. To overcome these effects, annular specimens have been proposed [34, 35]. The use of pulse shaping, in which the rise time of the loading stress wave is increased and hence the acceleration imposed on the specimen decreased, is also effective in reducing the amount of ringing, and also the strain accumulated in the specimen during this time [36]. The low absolute strength of many polymers and biomaterials also causes challenges. Compared to a metallic Hopkinson bar, very low forces may be supported, and the low amplitude stress waves in the bars are difficult to measure. This can be overcome by low stiffness (and low impedance) bars such as magnesium alloy, polymer (often called viscoelastic) [37-40] or hollow metal [41] (see also [25, 42]). The latter two require careful calibration because wave propagation is dispersive, leading to pulse attenuation (in polymer bars) and phase changes (in both) between the specimen and the bar instrumentation; there is a substantial body of literature on this subject [43-45]. In addition, more sensitive stress gauges, quartz or PZT, may be used; these can also provide a useful direct measurement of the stress at both ends of the specimen [36, 46, 47].

For rubber specimens large strains are required to fully characterize the hyperelastic response. In principle, the useful duration of an experiment is determined by the length of the Hopkinson bar system [48], but ever increasing lengths are not usually feasible. Some advantage can be gained by using multiple gauge stations on the bars so that longer stress-waves can be used: although the waves overlap they can be separated into input and reflected waves as long as sufficient gauge locations are used [49-51]. Direct impact Hopkinson bars, in which there is no input bar, also give longer loading durations, can achieve higher strain rates, and allow the apparatus to be elongated because only the output bar is required [2, 3, 52]. This comes at the expense of not being able to measure the force on the front face of the specimen. Another approach, combining elements of the above, is to directly measure the forces at the bar-specimen interface using stress gauges, and the length of the specimen optically, so that the bars become waveguides to load the specimen only: not to transmit information between the specimen and gauges [53].

Most Hopkinson bar data on polymers deal with compressive loading only. Accurate measurements of the tensile response face similar difficulties, and often more so, because uniaxial tensile tests usually require a specimen with a large length to diameter ratio, which precludes short specimens. Studies include [11, 54-59]. The difficulties of achieving large strains, or conversely of dealing with brittle specimens still exist, although these can be alleviated using carefully controlled long duration loading and pulse shaping [60-63] and high speed imaging combined with finite element modelling can allow more information to be obtained about the constitutive behavior of the specimens [64].

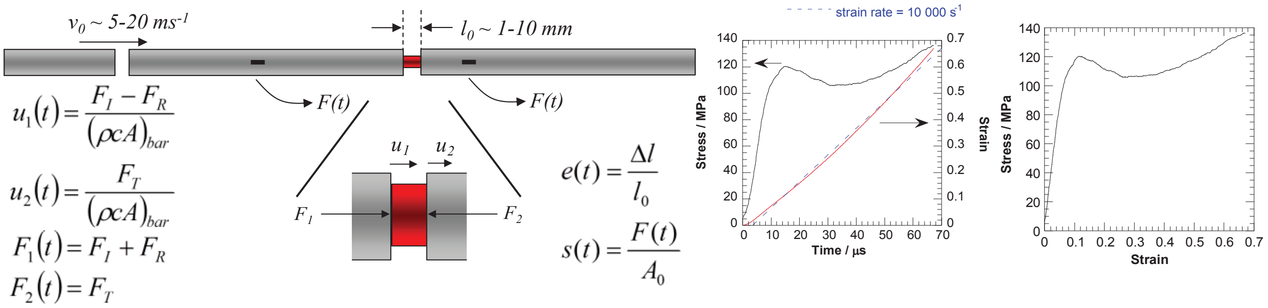

FIGURE 5. Schematic diagram of split Hopkinson bar, basic data analysis equations and output stress-strain curve for a polycarbonate specimen at 10 000 s^{-1}, room temperature.

Other techniques

For strain rates lower than ca. 500 s^{-1}, a number of techniques have been used, including drop-weights [4, 65-71], flywheel systems [72, 73], the expanding ring technique [74], the cam plastometer [75] and the innovative wedge bar [76-78]. Below about 10 s^{-1} it is reasonable to expect to design a loading apparatus and specimen for which the natural frequency of both is sufficiently higher than the frequencies required in the loading that no oscillations occur. Between 10 and 500 s^{-1}, the choice is whether to use one of these apparatus (e.g. [79]), or to design and build a long duration Hopkinson bar system [48], or a hybrid system [80]. There have also been attempt to measure fracture properties under dynamic loading (e.g. [81-85]), and dynamic pull-out stresses for fibers embedded in polymer systems [86]. For higher rates, plate impact techniques may be used to measure the shock response [10, 13, 87-95].

Returning to the 'high rate' response between 100 and 10 000 s^{-1}, further techniques exist in which static equilibrium is *not* required. Two well-established techniques are discussed in this section, whilst further more recently developed methods are discussed below.

Taylor Impact and Dynamic Tensile Extrusion

Taylor Impact was first described in 1946 as a means of measuring the dynamic yield strength of metals [96, 97]. Its key advantage at the time was that no in-situ real-time measurements are required. A slender rod of material is impacted at high speed into an approximately rigid anvil (or into a second, identical rod: the symmetric Taylor Impact [98]). The specimen is recovered, and an assessment of the region over which plastic deformation has occurred is made. Using the initial and final lengths, and the length of the plastic deformation, Taylor produced an analysis to derive the dynamic yield strength. It was later realized that this analysis was inappropriate for polymeric materials, and a modified analysis was developed by Hutchings [99, 100]; owing to viscoelastic recovery after loading high speed photography should be used. A feature of the Taylor Impact is that stresses, strain rates and final strains vary within a single specimen. Whilst this is a disadvantage for measuring yield strengths, a more common use of the Taylor impact is to test constitutive models: for which the more complex loading is thought to provide a more robust test [18]. In this case, high speed photography can provide a useful time-resolved measurement of specimen geometry for comparison to the model of interest [101-103]. Another use of Taylor Impact is to obtain information about the ductile to brittle response in polymers, e.g. in PFTE [12, 13] and other polymers [8, 104-107]

More recently, similar transitions in polymer response, this time in tension, have been investigated using the dynamic tensile extrusion experiment, in which a polymer sphere or rod is impacted at high speed into a converging nozzle. The polymer is then observed using high speed photography as it exits the nozzle; recent data have shown that this test is sensitive to the ductility of the specimen material [108-114].

Transverse Impact

Characterization of fibers offers further challenges, as they can often combine high intrinsic material strength with low sample strength. However, with growing use of fiber reinforced composites and interest in biomaterials such as silk, interest in the dynamic response of fibers is increasing. A long-standing method for testing this response is transverse impact [115, 116]. Here, a fiber is suspended from one end, and tensioned, usually by means of a small mass at the other end. The fiber is impacted by a wedge-ended projectile in a direction perpendicular to the fiber length. The impact induces a longitudinal wave, which travels rapidly along the fiber and causes a change in the stress and strain in the material. There is also a transverse wave, which follows more slowly. Because the transverse wave speed is a function of the fiber density and tension only (and not the other mechanical properties) this speed gives information about the stress induced by the preceding longitudinal wave. Furthermore, the transverse wave takes up the strain induced by the longitudinal deformation. Hence, by means of high speed photography, both the stress and strain in the fiber can be calculated. From this information, stress-strain curves can be calculated by either varying the impact speed or by varying the pre-tension. The analysis is discussed further in a recent silk paper [117].

The main drawback of this technique, especially for biomaterials, is that long specimens are required: the analysis requires that the longitudinal wave does not return from the top support until sufficient measurements of the transverse wave position have been made. Authors have also measured fiber properties in suitably modified Hopkinson bar (e.g. [118]) or using gas gun loading (e.g. [119]).

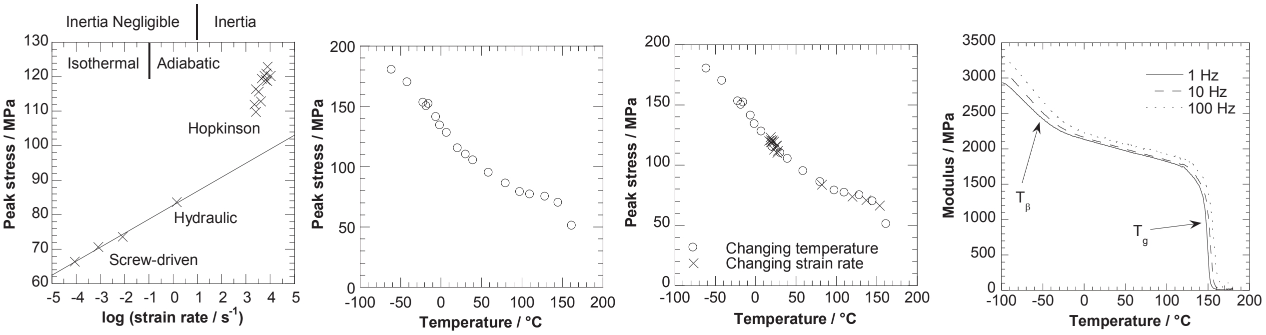

(a) (b) (c) (d)

FIGURE 6. (a) Dependence of yield stress on strain rate in Polycarbonate at ca. 20 °C, showing the increased rate dependence at higher strain rates and indicating some of the factors which affect interpretation; (b) dependence of yield stress on temperature at ca. 5000 s^{-1}; (c) mapping rate dependence onto temperature dependence; (d) DMTA data showing temperature dependence of modulus at three frequencies [5, 120].

STRAIN RATE DEPENDECE IN POLYMERS

Overview

A number of studies have presented data on the mechanical response of polymers, as quantified by the stress-strain relationship, as a function of applied strain rate. Indeed, the first data on polymer response in a split-Hopkinson bar was presented in the first paper on the split-bar: Kolsky's 1949 paper included data from polythene and natural rubber, whilst the 1964 paper by Davies and Hunter presented data on PMMA, PVC, PC, PTFE and rubber [31, 32] (see also [97]). Already, Kolsky was worried about equilibrium effects, and used short specimens, between 0.3 and 3 mm long. Further data were published on various materials, and in 1994 a wide-ranging study by Walley and Field presented data from ca. 10^{-3} to 10^{4} s^{-1} on a large number of polymers, with stress-strain relationships obtained at nearly every decade of strain rate [3]. As was, and is, common, the behavior was parameterized by the yield strength, which was then plotted against log(strain rate), a so-called Eyring plot [1].

A common feature of polymers is that the strain rate sensitivity is larger at higher rates, Fig. 6. This has been observed by a number of authors on a wide range of polymer materials. However, careful interpretation is required for three reasons. Firstly, similar results are also seen in other materials [121, 122]. Secondly, the relevant strain rates are often also those at which inertial effects become important: if the specimen is too large, the stress induced by the specimen inertia can become significant compared to the intrinsic material strength [33]. Thirdly, the change in rate sensitivity typically occurs when the test equipment changes from screw driven or hydraulically driven devices to Hopkinson bars. However, the interpretation of these data gives an example of the importance of integrating rate and temperature dependence of polymeric materials and is discussed in the next section.

Whilst this paper, discusses mainly the compressive response at high strain rates, investigations of other behavior are available in the literature. These include tensile and shear behavior, the Mullins effect (e.g. [62, 123]), the effect of confining pressure, volume and temperature changes during loading, and dynamic fracture.

Rate and Temperature Effects

Uniquely, polymers allow data interpretation through time-temperature superposition. By performing experiments over a range of strain rates at a single temperature, and a range of temperatures at a single strain rate, and noting that increasing log(strain rate) is equivalent to decreasing temperature, the data at fixed temperatures can be mapped onto those at fixed rates (or vice versa). These mapped results can then be compared to other, well-established, methods for measuring the thermo-mechanical response of polymers, e.g. DMTA, Fig. 6. In this way, it has been established that the observed increase in rate sensitivity of amorphous or semi-crystalline polymers is an effect of underlying polymer transitions which would normally be observed below room temperature (typically the β transition), but which shift to room temperature as the strain rate increases. The first use of this technique to interpret rate dependence of yielding behavior was probably by Rinde, Bauwens and Bouwens-Crowet [124-126]: a master curve of rate dependence extending outside the range of experimentally accessible rates was calculated. More recently this approach has been applied to a number of materials: PC and PVDF [5], PTFE [127], PE [128], Polymer bonded explosives [4, 129] and PVC [17] (see also a recent discussion of different shifting methods [130]). It should be noted that for rubbery materials with a glass transition close to room temperature, the effect of this transition would be expected to be seen, and is seen, in the rate dependence. However, because the range of strain rates which can be accessed experimentally is small compared to the equivalent range of temperatures, it is rare to be able to observe the effects of more than one transition in a single polymer through strain rate alone [17]. A related approach has been used very successfully to develop models for high rate behavior [131].

Having used time-temperature superposition to interpret high rate data, a logical extension is to replicate high rate material behavior in low rate experiments. This gives the opportunity to design a framework in which the full range of available diagnostics can be applied in the low rate experiments but used to interpret the high rate response. A necessary step is to separate the intrinsic rate dependence of the polymer from the effects of dynamic loading. The effects of inertia have already been discussed; they can be quantified using well-established equations and then minimized in the high rate experiments [33, 35]. A second difference between static and dynamic loading is specimen heating. Some proportion of the plastic work done on the specimen is converted to heat: at low strain rates this heat has time to conduct out of the specimen so the experiment is isothermal; at sufficiently high rates the heat remains in the specimen and the experiment is adiabatic. The transition between the two depends on the thermal diffusivity of the material and the specimen dimensions; although it is in fact a gradual transition, it should be remembered that the rate dependence is in log(strain rate), so compared to the change in intrinsic response, the transition from isothermal to adiabatic may still be quite sharp [120, 132].

Recently, research has been performed in which the high strain rate response of PVC, PC and PMMA is simulated in a low rate experiment, which would otherwise be isothermal, by profiling the temperature during the experiment, Fig. 7. Firstly, the yield stress is replicated by appropriately reducing the ambient temperature. Then, the temperature is gradually increased during the experiment to simulate some fraction of plastic work being converted to heat, and that heat remaining in the specimen. For PVC this was found to faithfully replicate the high rate response. For PC and PMMA the response could be replicated, but only by varying the amount of 'work converted to heat' [120, 132]. Whilst further research is required to sort this out, it is clear that this technique offers opportunities to better understand the underlying mechanisms governing rate dependence, and also to replicate high rate response of composite systems through highly instrumented low rate experiments.

A related experimental approach is to carefully obtain an isothermal stress-strain response by loading a specimen in stages, each time the specimen is allowed to yield and undergo a small amount of plastic deformation before the experiment is stopped; the specimen is allowed to cool before reloading [130]. This technique has also been used on metals [133]. This provides stress-strain relationships which are clearly different from those obtained through monotonic loading, and works best for intermediate rate loading where there is sufficient control of the loading device that the experiment can be stopped and restarted as required.

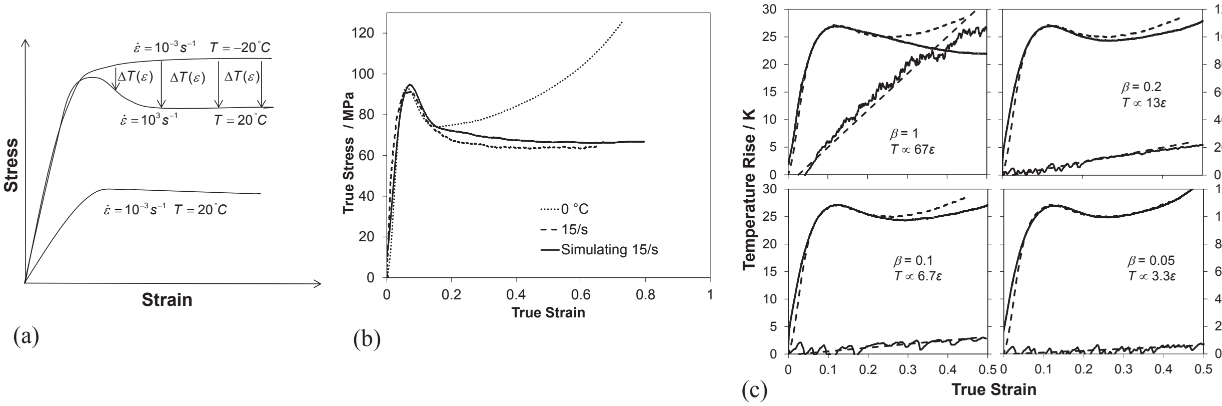

(a)

(b)

(c)

FIGURE 7. Simulating the high rate response of a polymer using low rate experiments with temperature profiles. (a) Illustration of the concept, by performing a quasi-static experiment initially at reduced temperature (to reproduce yield) and then increasing the temperature as a function of strain to simulate adiabatic heating; (b) Experimental data from simulating the room temperature behavior of PVC at 15 s^{-1} using by loading at 10^{-2} s^{-1} initially at 0 °C, comparison also to the isothermal 0 °C response showing the very different post-yield behavior [132]; (c) For polycarbonate, the simulation works if only a small amount of work is assumed to be converted to heat, the so-called β factor [120].

FURTHER TECHNIQUES USING WAVE PROPAGATION

Background

One of the key difficulties of the Hopkinson bar technique, especially for soft materials, is the requirement for the specimen to be in quasi-static equilibrium in order for stress-strain relationships to be calculated. The main reason for this is that only surface measurements of force are made. One way to address this issue is to use finite element models of the bar-specimen system, outputs from which can be directly compared to the strain gauge signals from an experiment (without the requirement to reconstruct the stress-strain relationship in the specimen, which makes assumptions about both the specimen behavior and the wave propagation in the bars themselves). This is a particularly powerful technique for validating material models, as imperfections in the loading, effects due to wave dispersion in the loading rod, and those due to wave propagation in the specimen, which would otherwise need to be minimized or corrected, become part of a more complex and hence challenging loading regime, which must then be replicated by the model [134].

Another approach is to use approaches in which the wave propagation characteristics in an extended specimen are used to calculate material properties. This is similar to the approach in the transverse technique outlined above, and in the techniques used to measure shock response of materials. Wave propagation may be monitored by strain gauges, high speed photography and laser velocimetry, amongst other methods.

Methods with high speed photography

Modern digital high speed cameras offer suitable combinations of framing rate, resolution and noise to monitor the displacements induced when stress waves propagate through materials [135]. It can easily be shown that the displacements, wave-speeds and strains are consistent with the material response [136], and hence, if sufficient measurements can be made, it should be possible to use an inverse methodology to derive the material properties from suitable measurements of wave propagation parameters. One method is to compare the observed strain and particle velocity to that predicted from a suitable constitutive model [137-139]. However, as well as calculating strains directly from displacements, if the images can be obtained with sufficient time resolution, it is also possible to calculate velocities and accelerations, and hence to calculate stress fields: the inertia of the specimen itself is used as a dynamic load cell.

Here we consider the problem of a thin rectangular specimen, which may be assumed to experience plane stress conditions when dynamically loaded from one end. In order to calculate absolute stress fields, two approaches may be used. One is to ensure that the specimen has a free end (or at least an end where the stress is known): by integrating the acceleration from this end it is then possible to derive the stress field in the specimen. An example of this approach is given in Pierron *et al.* [140], in which a gas gun was used to impact flat quasi-isotropic composite plates with a steel projectile. The stress wave (and accompanying displacement, strain and acceleration fields) were measured using high speed imaging of a grid bonded to the specimen surface. From the boundary condition that the stress was zero on the free edges, stress fields were also calculated, allowing calculations of the modulus as a function of strain throughout the duration of the loading.

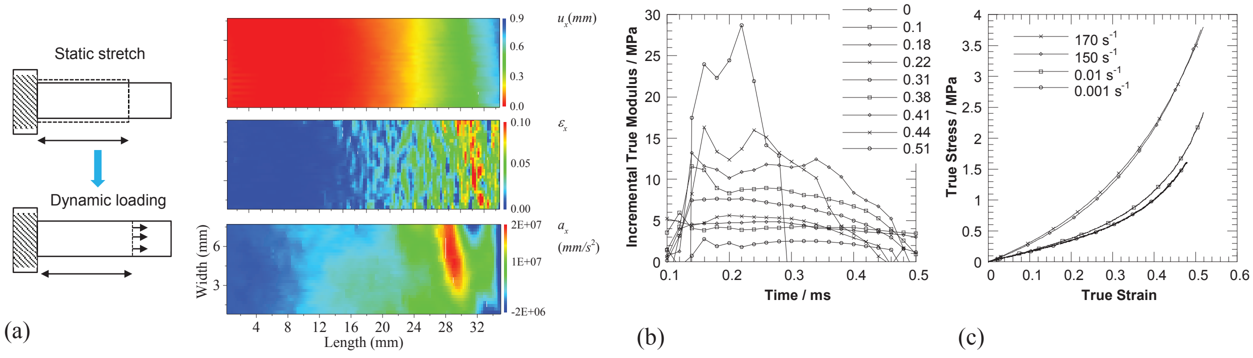

FIGURE 8. Application of Virtual Fields Method to dynamic loading of an elastomer: (a) loading scheme and example of displacement, strain and acceleration fields; (b) incremental dynamic modulus increases as a function of static pre-stretch; (c) stress strain curve obtained compared to those calculated from quasi-static loading [141].

The second method is to use the Virtual Fields Method (VFM, also used in [140]). This method, which is an extension of the principle of virtual work, enables the effects of the externally applied forces on the specimen boundaries to be cancelled so that the strains and accelerations within the specimens may be used to calculate appropriate material parameters. A complete description of the method may be found in a recent book [142], and a discussion of its application in dynamic experiments in a number of papers [143-146]. Recently, the VFM has been applied to hyperelastic rubber specimens, to obtain constitutive parameters at strain rates of about 200 s^{-1} in tension. In order to obtain strain hardening parameters data at large strains are required; however, it is experimentally challenging to introduce large amplitude stress waves without either increasing the strain rate unduly, or risking shock wave formation. In this case, therefore, large amplitude response was obtained by the use of static pre-deformations, Fig. 8. For each pre-deformation the local dynamic stiffness was obtained using high speed photography and digital image correlation on random speckle patters on the specimen surface. This modulus was assumed to be the local tangent stiffness to the stress-strain curve, so that multiple measurements allow the constitutive parameters to be obtained. It is noted that so-far the strain rates obtained are lower than those from the Hopkinson bar techniques described above: development of higher strain rate techniques is ongoing [141].

Methods with strain gauges

The propagation of a stress wave in a slender rod is described by the solution to a wave equation, and parameterized by the propagation coefficient, itself a combination of the wave number and the attenuation coefficient. Both of these may in turn be calculated from material parameters (for elastic or linear viscoelastic materials, the complex modulus and density) and the bar dimensions [45, 147]. Frequency dependence comes in two forms, from the material parameters and the inertial effects of the bar itself, which causes wave dispersion described by the Pochhammer-Chree equations and their solutions [148, 149]. For the latter, dispersion becomes most significant for wavelengths of about 10 bar diameters or less, although the exact effects depend on the ratio of the bar materials' density and modulus. More detailed descriptions can be found in the literature, e.g. [150-155].

Hence, by measuring the phase and amplitude of an arbitrary wave as it propagates along a slender rod, if the inertia driven dispersion is sufficiently small, or can be corrected [156], the wavenumber can be obtained and used to derive material properties [157, 158]. By performing the analysis on Fourier transforms of the wave signals, this can also be done as a function of frequency. Having obtained the wave profiles from strain gauge signals, the key challenges are to select and FFT the pulses, whilst retaining the full phase information. This technique has been successfully used to obtain frequency dependent viscoelastic properties up to frequencies of ca. 20 kHz. However, although modern data acquisition and processing hardware make the technique easier to apply, just as the split-Hopkinson bar, this techniques was also first used by Kolsky to derive properties of rubbers [159].

SUMMARY AND CONCLUSIONS

The rate dependence of polymers has been of interest from the earliest days of high strain rate testing, and indeed many of the techniques we use today (including the split-Hopkinson bar and wave propagation techniques) were first used by Kolsky on polymers in the 1940s. Over the past 20 years, there has been great development in loading and instrumentation techniques which allow the high rate response of polymers, including elastomers, to be measured with increasing accuracy. The observed response shows the familiar relationships with temperature, allowing time-temperature superposition to be used to interpret the rate dependence, as was first illustrated in the 1970s. Polymers are also suited to measurements using wave propagation parameters, either through optical or contacting measurements of the strains and accelerations in specimens during this propagation, although further development of these techniques is almost certainly required.

ACKNOWLEDGEMENTS

The author would like to thank the following people with whom he has performed polymer research over the past 12 years: JE Field, SM Walley (also for reading an earlier draft of this manuscript and providing very useful suggestions), WG Proud, DM Williamson, S Palmer, M Kendall, B Mortimer, DR Drodge, S-H Yoon, Y Huang, X Tang (in particular for providing the data in Fig. 2), JL Jordan, J Foley, R Froud and R Duffin. He also acknowledges the financial support of AFOSR (FA8655-09-1-3088 and FA8655-12-1-2015) and EPSRC (EP/J011436/1) and of Pembroke College, Oxford.

REFERENCES

1. S.M. Walley, J.E. Field, P.H. Pope, and N.A. Safford, J Phys III France 1 **1**(12), 1889-1925 (1991).
2. S.M. Walley, J.E. Field, P.H. Pope, and N.A. Safford, Phil.Trans. R. Soc. A. **328**(1597), 1-33 (1989).
3. S.M. Walley and J.E. Field, DYMAT Journal **1**, 211-228 (1994).
4. D.M. Williamson, C.R. Siviour, W.G. Proud, S.J.P. Palmer, R. Govier, K. Ellis, P. Blackwell, and C. Leppard, J. Phys D: Appl. Phys. **41**(8), 085404 (2008).
5. C.R. Siviour, S.M. Walley, W.G. Proud, and J.E. Field, Polymer **46**(26), 12546-12555 (2005).
6. P.J. Rae and D.M. Dattelbaum, Polymer **45**(22), 7615-7625 (2004).
7. M.L. Williams, R.F. Landel, and J.D. Ferry, J. Am. Chem. Soc. **77**(14), 3701-3707 (1955).
8. E.N. Brown, P.J. Rae, and E.B. Orler, Polymer **47**(21), 7506-7518 (2006).
9. E.N. Brown, P.J. Rae, E.B. Orler, G.T. Gray, and D.M. Dattelbaum, Mat. Sci. Eng., C **26**(8), 1338-1343 (2006).
10. E.N. Brown, C.P. Trujillo, G.T. Gray, P.J. Rae, and N.K. Bourne, J. Appl. Phys. **101**(2), 024916 (2007).
11. P.J. Rae and E.N. Brown, Polymer **46**(19), 8128-8140 (2005).
12. P.J. Rae, E.N. Brown, B.E. Clements, and D.M. Dattelbaum, J. Appl. Phys. **98**(6), 063521 (2005).
13. N.K. Bourne, E.N. Brown, J.C.F. Millett, and G.T. Gray, III, J. Appl. Phys. **103**(7), 074902 (2008).
14. R. Gerlach, C.R. Siviour, N. Petrinic, and J. Wiegand, Polymer **49**(11), 2728-2737 (2008).
15. O.A. Shergold, N.A. Fleck, and D. Radford, Int. J Impact Eng. **32**(9), 1384-1402 (2006).
16. M.F. Ashby, Acta Metallurgica **37**(5), 1273-1293 (1989).
17. M.J. Kendall and C.R. Siviour, Proc. R Soc. A **470**(2167), 20140012 (2014).
18. J.E. Field, S.M. Walley, W.G. Proud, H.T. Goldrein, and C.R. Siviour, Int. J. Impact Eng. **30**(7), 725-775 (2004).
19. S.M. Walley, W.G. Proud, P.J. Rae and J.E. Field, "The dynamic temperature measurement of split Hopkinson bar specimens using small thermocouples and infrared streak photography" in *Dymat 2009: 9th International Conference on the Mechanical and Physical Behaviour of Materials under Dynamic Loading,* Vol 1, 511-516 (2009).
20. M.J. Kendall, R.F. Froud, and C.R. Siviour, Polymer **55**(10), 2514-2522 (2014).
21. S.M. Walley, W.G. Proud, P.J. Rae, and J.E. Field, Rev. Sci. Instrum. **71**(4), 1766-1771 (2000).
22. A.T. Zehnder, P.R. Guduru, A.J. Rosakis, and G. Ravichandran, Rev. Sci. Instrum. **71**(10), 3762-3768 (2000).
23. P.R. Guduru, A.T. Zehnder, A.J. Rosakis, and G. Ravichandran, Eng. Fract. Mech. **68**(14), 1535-1556 (2001).
24. G.T. Gray III, *Classic split-Hopkinson pressure bar testing*, in *ASM Handbook. Vol. 8: Mechanical Testing and Evaluation*, H. Kuhn and D. Medlin, Editors. 2000, ASM International: Materials Park, Ohio. p. 462-476.
25. G.T. Gray III and W.R. Blumenthal, *Split-Hopkinson pressure bar testing of soft materials*, in *ASM Handbook. Vol. 8: Mechanical Testing and Evaluation*, H. Kuhn and D. Medlin, Editors. 2000, ASM International: Materials Park, Ohio. p. 488-496.
26. W.N.W. Chen and B. Song, *Split Hopkinson (Kolsky) Bar: Design, Testing and Applications* (Springer, New York, 2011).
27. K.T. Ramesh, "High Rate and Impact Experiments", in *Springer Handbook of Experimental Solid Mechanics*, edited by W.N.J. Sharpe (Springer, New York, 2008) pp. 929-960.
28. W. Chen, F. Lu, D.J. Frew, and M.J. Forrestal, J. Appl. Mech.- T. ASME **69**(3), 214-223 (2002).
29. C.R. Siviour, "High strain rate properties of materials using Hopkinson bar techniques" PhD Thesis, Cambridge University 2005.
30. B.J. Briscoe and R.W. Nosker, Wear **95**(3), 241-262 (1984).
31. H. Kolsky, Proc Phys Soc Lond B **62**, 676-700 (1949).
32. E.D.H. Davies and S.C. Hunter, J. Mech. Phys. Solids **11**(3), 155-179 (1963).
33. D.A. Gorham, J. Phys. D: Appl. Phys. **22**, 1888-1893 (1989).
34. B. Song, Y. Ge, W.W. Chen, and T. Weerasooriya, Exp. Mech. **47**(5), 659-670 (2007).
35. M.J. Forrestal, T.W. Wright, and W. Chen, Int. J. Impact Eng **34**(3), 405-411 (2007).
36. W. Chen, F. Lu, and B. Zhou, Exp. Mech. **40**(1), 1-6 (2000).
37. H. Zhao, G. Gary, and J.R. Klepaczko, Int. J. Impact Eng **19**(4), 319-330 (1997).
38. H. Zhao and G. Gary, J. Mech. Phys. Solids **45**(7), 1185-1202 (1997).
39. L.L. Wang, K. Labibes, Z. Azari, and G. Pluvinage, Int. J. Impact Eng. **15**(5), 669-686 (1994).

40. O. Sawas, N.S. Brar, and R.A. Brockman, Exp. Mech. **38**(3), 204-210 (1998).
41. W. Chen, B. Zhang, and M.J. Forrestal, Exp. Mech. **39**(2), 81-85 (1999).
42. T.P.M. Johnson, S.S. Sarva, and S. Socrate, Exp. Mech. **50**(7), 931-940 (2010).
43. J.J. Harrigan, B. Ahonsi, E. Palamidi, and S.R. Reid, Phil. Trans. R. Soc. A **372**(2023) (2014).
44. M. Aleyaasin and J.J. Harrigan, Int. J Mech. Sci. **52**(5), 754-757 (2010).
45. B. Ahonsi, J.J. Harrigan, and M. Aleyaasin, Int. J. Impact Eng. **45**, 39-51 (2012).
46. R.J. Wasley, K.G. Hoge, and J.C. Cast, Rev. Sci. Instrum. **40**(7), 889 (1969).
47. M.J. Kendall, D.R. Drodge, R.F. Froud, and C.R. Siviour, Meas. Sci. Technol. **25**(7), 2514-2522 (2014).
48. B. Song, C.J. Syn, C.L. Grupido, W. Chen, and W.Y. Lu, Exp. Mech. **48**(6), 809-815 (2008).
49. Z. Han and G. Gary, J. Mech. Phys. Solids **45**(7), 1185-1202 (1997).
50. C. Bacon, Int. J. Impact Eng. **22**(1), 55-69 (1999).
51. J. Shim and D. Mohr, Int. J. Impact Eng. **36**(9), 1116-1127 (2009).
52. S. Hiermaier and T. Meenken, J. Strain Anal. Eng. Des. **45**(6), 401-409 (2010).
53. R. Chen, S. Huang, K. Xia, and F. Lu, Rev. Sci. Instrum. **80**(7), 076108 (2009).
54. C. Kan, W. Yang, and W. Yu, Int. J. Solids Struct. **51**(13), 2539-48 (2014).
55. S. Fu, Y. Wang, and Y. Wang, Polymer Testing **28**(7), 724-729 (2009).
56. J.T. Fan, J. Weerheijm, and L.J. Sluys, Polymer **65**, 72-80 (2015).
57. W. Chen, F. Lu, and M. Cheng, Polymer Testing **21**(2), 113-121 (2002).
58. K. Cao, Y. Wang, and Y. Wang, Materials & Design **38**, 53-58 (2012).
59. M. Foster, B. Claus, N. Parab, B. Lim, W. Chen, T. Sun, K. Fezza, Journal of Dynamic Behavior of Materials **1**(2), 162-175 (2015).
60. R. Gerlach, S.K. Sathianathan, C. Siviour, and N. Petrinic, Int. J. Impact Eng. **38**(12), 976-980 (2011).
61. R. Gerlach, C. Kettenbeil, and N. Petrinic, Int. J. Impact Eng. **50**, 63-67 (2012).
62. M. Cheng and W.N. Chen, Int. J. Solids Struct. **40**(18), 4749-4768 (2003).
63. X. Nie, B. Song, Y. Ge, W.W. Chen, and T. Weerasooriya, Exp. Mech. **49**(4), 451-458 (2009).
64. S.S. Sarva and M.C. Boyce, J. Mech. Mater. Struct. **2**(10), 1853-1880 (2007).
65. J. Cai, S.M. Walley, R.J.A. Hunt, W.G. Proud, V.F. Nesterenko, and M.A. Meyers, Mat. Sci. Eng., A **472**(1-2), 308-315 (2008).
66. M.L. Dannis and R.E. Watling, Rev. Sci. Instrum. **37**(12), 1716 (1966).
67. O. Ramon, S. Mizrahi, and J. Miltz, Polym. Eng. Sci. **34**(18), 1406-1410 (1994).
68. G.M. Swallowe and S.F. Lee, J. Phys. IV **110**, 33-38 (2003).
69. S.F. Lee and G.M. Swallowe, Imaging Sci. J. **52**(4), 193-201 (2004).
70. A. Trautmann, C.R. Siviour, S.M. Walley, and J.E. Field, Int. J. Impact Eng. **31**(5), 523-544 (2005).
71. J.E. Balzer, C.R. Siviour, S.M. Walley, W.G. Proud, and J.E. Field, Proc. R. Soc. A **460**(2043), 781-806 (2004).
72. P. Viot, F. Beani, and J.L. Lataillade, J. Mat. Sci. **40**(22), 5829-5837 (2005).
73. J.S. Foot, R.W. Truss, I.M. Ward, and R.A. Duckett, J. Mat. Sci. **22**(4), 1437-1442 (1987).
74. N.S. AlMaliky and D.J. Parry, Meas. Sci. Technol. **7**(5), 746-752 (1996).
75. F. Scarpa, L.G. Ciffo, and J.R. Yates, Smart Mater. Struct. **13**(1), 49-56 (2004).
76. T.J. Cloete and M. Stander, EPJ Web of Conferences **26**, 01025 (6 pp.)-01025 (6 pp.) (2012).
77. T.J. Cloete, G. Paul, and E.B. Ismail, Phil. Trans. R. Soc. A **372**(2015) (2014).
78. T.J. Cloete and S. Oxtoby "A new technique for compression tests at intermediate strain rates: Prototype results" in *Dymat 2009: 9th International Conference on the Mechanical and Physical Behaviour of Materials under Dynamic Loading,* Vol 1. 249-255 (2009).
79. P.H. Mott, J.N. Twigg, D.F. Roland, H.S. Schrader, J.A. Pathak, and C.M. Roland, Rev. Sci. Instrum. **78**(4) (2007).
80. M.M. LeBlanc and D.H. Lassila, Exp. Techniques **20**(5), 21-24 (1996).
81. S.N. Wosu, D. Hui, and P.K. Dutta, Eng. Fract. Mech. **72**(10), 1531-1558 (2005).
82. S. Dong, Y. Wang, and Y. Xia, Polymer Testing **25**(7), 943-952 (2006).
83. H. Koerber, J. Xavier, and P.P. Camanho, Mech. Mater. **42**(11), 1004-1019 (2010).
84. C.T. Sun and C. Han, Composites Part B **35**(6-8), 647-655 (2004).
85. T. Kusaka, M. Hojo, Y.W. Mai, T. Kurokawa, T. Nojima, and S. Ochiai, Compos. Sci. Technol. **58**(3-4), 591-602 (1998).
86. R. Gerlach, A. Pabst, N. Petrinic, A. Hornig, J. Wiegand, C.R. Siviour, and W. Hufenbach, Compos. Sci. Technol. **69**(11-12), 2024-2026 (2009).

87. J.C.F. Millett, G. Whiteman, S.M. Stirk, and N.K. Bourne, J. Phys. D: Appl. Phys. **44**(18) (2011).
88. J.C.F. Millett, N.K. Bourne, and G.T. Gray, J. Phys. D: Appl. Phys. **37**(6), 942-947 (2004).
89. J.C.F. Millett, N.K. Bourne, and G.T. Gray, J. Appl. Phys. **96**(10), 5500-5504 (2004).
90. J.C.F. Millett and N.K. Bourne, J. Phys. D: Appl. Phys. **37**(20), 2901-2907 (2004).
91. J.C.F. Millett and N.K. Bourne, J. Phys. D: Appl. Phys. **9**(5), 2576-2579 (2001).
92. T. Jiao, R.J. Clifton, and S.E. Grunschel, "Pressure-sensitivity and tensile strength of an elastomer at high strain rates", in *Shock Compression of Condensed Matter - 2007*, edited by M. Elert, M.D. Furnish, R. Chau, N.C. Holmes, and J. Nguyen, (American Institute of Physics, Melville, NY, 2007). pp. 707-710.
93. T. Jiao and R.J. Clifton, "Measurement of the response of an elastomer at pressures up to 9 GPa and shear-rates of $10^5 – 10^6$ s^{-1}" J. Phys.: Conf. Ser. 500 112036 (2014)
94. N.K. Bourne, J.C.F. Millett, E.N. Brown, and G.T. Gray, III, J. Appl. Phys. **102**(6) (2007).
95. A.S. Abou-Sayed and R.J. Clifton, Transactions of the ASME. Series E, J. Appl. Mech. **44**(1), 79-84 (1977).
96. G.I. Taylor, Proc. R. Soc. A **194**(1038), 289-299 (1948).
97. G.I. Taylor, J. Inst. Civil Eng. **26**, 486-519 (1946).
98. D.C. Erlich, "Rod Impact (Taylor) Test", in *Metals Handbook Vol. 8 (9th edn.)*. . (American Society of Metals 1985) pp. 203-207.
99. B.J. Briscoe and I.M. Hutchings, Polymer **17**(12), 1099-1102 (1976).
100. I.M. Hutchings, J. Mech. Phys. Solids **26**(5), 289-301 (1978).
101. E. Wielewski, M.R. Arthington, C.R. Siviour, S. Carter, F. Hofmann, A.M. Korsunsky, and N. Petrinic, J. Strain Anal. Eng. Des. **45**(6), 429-437 (2010).
102. S. Sarva, A.D. Mulliken, and M.C. Boyce, Int. J. Solids Struct. **44**(7-8), 2381-2400 (2007).
103. H. Cho, S. Bartyczak, W. Mock, and M.C. Boyce, Polymer **54**(21), 5952-5964 (2013).
104. J.C.F. Millett, N.K. Bourne, and G.S. Stevens, Int. J. Impact Eng. **32**(7), 1086-1094 (2006).
105. P.J. Rae, E.N. Brown, and E.B. Orler, Polymer **48**(2), 598-615 (2007).
106. E.N. Brown, C.P. Trujillo, and G.T. Gray, III, "Influence of polyethylene molecular conformation on Taylor impact measurements: A comparison of HDPE, UHMWPE, and PEX", in *Shock Compression of Condensed Matter - 2007*, edited by M. Elert, M.D. Furnish, R. Chau, N.C. Holmes, and J. Nguyen (American Institute of Physics, Melville, NY, 2007). pp. 691-694.
107. A.D. Resnyansky, N.K. Bourne, E.N. Brown, J.C.F. Millett, P.J. Rae, S.A. McDonald, and P.J. Withers, J. Appl. Phys. **116**(22) (2014).
108. J. Furmanski, C.P. Trujillo, D.T. Martinez, G.T. Gray, and E.N. Brown, Polymer Testing **31**(8), 1031-1037 (2012).
109. C.P. Trujillo, E. Brown, and G. Gray, "Dynamic-tensile-extrusion response of polytetrafluoroethylene (PTFE). and polychlorotrifluoroethylene (PCTFE)", in *Dynamic Behavior of Materials.* 2011, Springer, pp. 73-75.
110. E.N. Brown, C.P. Trujillo, and G.T. Gray, III, "Dynamic-Tensile-Extrusion Response of Fluoropolymers" in *Shock Compression of Condensed Matter - 2009, edited by* M.L. Elert, W.T. Buttler, M.D. Furnish, W.W. Anderson, and W.G. Proud (American Institute of Physics, Melville, NY, 2009). pp. 1233-1236.
111. E.N. Brown, G.T. Gray, III and C.P. Trujillo "Influence of necking propensity on the dynamic-tensile-extrusion response of fluoropolymers." in *Dymat 2009: 9th International Conference on the Mechanical and Physical Behaviour of Materials under Dynamic Loading,* Vol 1. 2009. pp.171-177.
112. J. Furmanski, C. Cady, P. Rae, C.P. Trujillo, G.T. Gray, III, and E.N. Brown, "Dynamic-tensile-extrusion of polyurea" in *Shock Compression of Condensed Matter - 2011,* edited by M.L. Elert, W.T. Buttler, J.P. Borg, J.L. Jordan, and T.J. Vogler, (American Institute of Physics, Melville, NY, 2012).
113. E.N. Brown, J. Furmanski, K.J. Ramos, D.M. Dattelbaum, B.J. Jensen, A.J. Iverson, C.A. Carlson, K. Fezzaa, G.T. Gray, III, B.M. Patterson, C.P. Trujillo, D.T. Martinez, and T.H. Pierce "High-density polyethylene damage at extreme tensile conditions" J. Phys.: Conf. Ser. **500** 112011 (2014).
114. J. Furmanski, E.N. Brown, G.T. Gray III, C. Trujillo, D.T. Martinez, S. Bilyk and R. Becker, "Extreme tensile damage and failure in glassy polymers via Dynamic-Tensile-Extrusion", in *Dynamic Behavior of Materials*. 2014, Springer, pp. 107-112.
115. J.C. Smith, F.L. Mccrackin, H.F. Schiefer, W.K. Stone, and K.M. Towne, J. Res. Natl Stand. **57**(2), 83-89 (1956).
116. J.E. Field and Q. Sun, "A high-speed photographic study of impact on fibres and woven fabrics." in *19th International Congress on High-Speed Photography and Photonics, Pts 1 and 2,* edited by B. Garfield and J. Rendell. Vol. 1358. (1991) pp. 703-712.
117. D.R. Drodge, B. Mortimer, C. Holland, and C.R. Siviour, J. Mech. Phys. Solids **60**(10), 1710-1721 (2012)

118. M. Hudspeth, B. Claus, N. Parab, B. Lim, W. Chen, T. Sun and K. Fezza, Journal of Dynamic Behavior of Materials **1**(1), 55-64 (2015).
119. B.P. Russell, K. Karthikeyan, V.S. Deshpande, and N.A. Fleck, Int. J. Impact Eng. **60**, 1-9 (2013).
120. M.J. Kendall and C.R. Siviour, Philos. Trans. R. Soc. Lond, Ser. A. **372**(2015) (2014).
121. P.S. Follansbee, G. Regazzoni, and U.F. Kocks, "The transition to drag-controlled deformation in copper at high strain rates" in *Mechanical Properties at High Rates of Strain: Proceedings of the Third Conference on the Mechanical Properties of Materials at High Rates of Strain,* 71-80 (1984).
122. R.W. Armstrong and S.M. Walley, International Materials Reviews **53**(3), 105-128 (2008).
123. K. Nakai and T. Yokoyama, Journal of Dynamic Behavior of Materials **1**(1), 15-27 (2015).
124. C. Bauwens-Crowet, J. Mat. Sci. **8**(7), 968-979 (1973).
125. J.C. Bauwens, J. Mat. Sci. **7**(5), 577-& (1972).
126. J.A. Rinde and K.G. Hoge, J. Appl. Polym. Sci. **15**(6), 1377-& (1971).
127. J.L. Jordan, C.R. Siviour, J.R. Foley, and E.N. Brown, Polymer **48**(14), 4184-4195 (2007).
128. E.N. Brown, R.B. Willms, G.T. Gray, III, P.J. Rae, C.M. Cady, K.S. Vecchio, J. Flowers, and M.Y. Martinez, Exp. Mech. **47**(3), 381-393 (2007).
129. D.G. Thompson, R. DeLuca, and W.J. Wright, "Time-temperature superposition applied to PBX mechanical properties", in *Shock Compression of Condensed Matter - 2011,* edited by M.L. Elert, W.T. Buttler, J.P. Borg, J.L. Jordan, and T.J. Vogler, (American Institute of Physics, Melville, NY, 2012).
130. J. Furmanski, C.M. Cady, and E.N. Brown, Polymer **54**(1), 381-390 (2013).
131. A.D. Mulliken and M.C. Boyce, Int. J Solids Struct. **43**(5), 1331-1356 (2006).
132. M.J. Kendall and C.R. Siviour, Polymer **54**(18), 5058-5063 (2013).
133. B.D. Goldthorpe, A.L. Butler, and P. Church, J. Phys. IV **4**(C8), 471-476 (1994).
134. P. Church, R. Cornish, I. Cullis, P. Gould, and I. Lewtas, Phil. Trans. R. Soc. A. **372**(2023) (2014).
135. F. Pierron, R. Cheriguene, P. Forquin, R. Moulart, M. Rossi, and M. Sutton, "Performances and limitations of three ultra high-speed imaging cameras for full-field deformation measurements" in *Advances in Experimental Mechanics VIII*, edited by R.L. Burguete, M. Lucas, E.A. Patterson, and S. Quinn (2011). p. 81-86.
136. C.R. Siviour, Meas. Sci.Technol. **20**(6) (2009).
137. J. Niemczura and K. Ravi-Chandar, J. Mech. Phys. Solids **59**(2), 457-472 (2011).
138. J. Niemczura and K. Ravi-Chandar, J. Mech. Phys. Solids **59**(2), 442-456 (2011).
139. J. Niemczura and K. Ravi-Chandar, J. Mech. Phys. Solids **59**(2), 423-441 (2011).
140. F. Pierron, H. Zhu, and C. Siviour, Philos. Trans. R. Soc. Lond, Ser. A. **372**(2023) (2014).
141. S.-H. Yoon, I. Giannakopoulos, and C.R. Siviour, Int. J Solids Struct. **69–70**, 553-568 (2015).
142. F. Pierron and M. Grediac, *Virtual Fields Methods: Extracting Constitutive Mechanical Parameters From Full-field Deformation Measurements*. (Springer 2012).
143. F. Pierron, M.A. Sutton, and V. Tiwari, Exp.Mech. **51**(4), 537-563 (2011).
144. F. Pierron and P. Forquin, Strain **48**(5), 388-405 (2012).
145. R. Moulart, F. Pierron, S.R. Hallett, and M.R. Wisnom, Exp.Mech. **51**(4), 509-536 (2011).
146. C. Devivier, F. Pierron, and M.R. Wisnom, Composites Part A **48**, 201-218 (2013).
147. A. Benatar, D. Rittel, and A.L. Yarin, J. Mech. Phys. Solids **51**(8), 1413-1431 (2003).
148. L. Pochhammer, J. Reine Angew. Math. **81**, 324-336 (1876).
149. C. Chree, Quart. J. Pure Appl. Math. **21**, 287-298 (1886).
150. A. Tyas and Z. Ozdemir, Phil.Trans. R. Soc. A. **372**(2023) (2014).
151. H. Kolsky, Philosophical Magazine **1**(8), 693-& (1956).
152. Z. Han and G. Gary, J. Mech. Phys. Solids **43**(8), 1335-48 (1995).
153. R.M. Davies, Phil.Trans. R. Soc. A. **240**(821), 375-457 (1948).
154. S.P. Anderson, Journal of Sound and Vibration **290**(1-2), 290-308 (2006).
155. H. Kolsky, *Stress Waves in Solids*. Clarendon Press, Oxford, 1953.
156. C. Bacon, Exp. Mech. **38**(4), 242-249 (1998).
157. S. Mousavi, D.F. Nicolas, and B. Lundberg, Journal of Sound and Vibration **277**(4-5), 971-986 (2004).
158. B. Lundberg and R.H. Blanc, Journal of Sound and Vibration **126**(1), 97-108 (1988).
159. K.W. Hillier and H. Kolsky, Proceedings of the Physical Society. Section B **62**(2), 111 (1949).